Proc. Indian Acad. Sci. (Earth Planet. Sci.), Vol. 103, No. 4, December 1994, pp. 449–468.

Incipient vortex size-dependent evolution of tropical disturbances Part II – Some governing processes

R KOTESWAR RAO and P GOSWAMI

CSIR Centre for Mathematical Modelling and Computer Simulation, Bangalore 560037, India

MS received 7 October 1993; revised 14 September 1994

Abstract. Recently it was shown (Goswami and Rao 1993) that the process of intensification of tropical disturbances depends on the size of the incipient vortex in a rather nonlinear fashion. Among vortices of size ranging from 100 to 450 km (radius), embedded in the same large scale condition, it is the vortex with size about 250 km that intensifies to the most severe system. These results also showed a strong correspondence between the maximum intensity reached and the initial (3–6 hour) low level convergence field near the centre. The purpose of the present work is to identify the process(es) responsible for this scale selective intensification of tropical disturbances. It is proposed that diffusion is likely to play a crucial role in bringing about this selective intensification. In the present work a series of experiments with an axisymmetric numerical model of tropical cyclone (Wada's model) is carried out to determine the relative roles of horizontal diffusion of momentum, moisture, heat and vertical diffusion. The results show that diffusion significantly affects the process of intensification and scale selection. While moderate diffusion does not alter the magnitude of intensification significantly, the scale selection is quite sensitive to the strength of diffusion. Interestingly, these diffusion processes, of momentum, moisture, heat and vertical do not affect the scale selection in the same fashion. The scale selection process turns out to be a result of a combined effect of these diffusion processes. However, no single diffusion process alone can give rise to a sharp selection of scale at the size of 250 km.

Keywords. Tropical cyclone; intensification; incipient vortex; scale selection; selective intensification; diffusion.

1. Introduction

Early detection and identification of potential cyclones in coastal localities can provide a significant boost to the efforts to issue timely 'warnings' and 'alerts' and thus to avoid under-warning and over-warning costs (Southern 1987). In locations like the east coast of India and the north coast of Australia, cyclogenesis often takes place within a few hundred kilometres from the coast, thus leaving a very short interval of time between its formation and the landfall. In the North Indian Ocean basins the problem is further compounded by the fact that many systems intensify in about 12 hours or less (Frank 1987), giving very little time to act. A great part of the problem could be solved, however, if one could identify a potential cyclone at an early stage. Since the tropical cyclones form from initial convective disturbances like cloud clusters or mesoscale convective complexes, identifying a potential cyclone at an early stage would imply identifying a potentially intensifying convective disturbance. Such a convective disturbance will need, in general, several parameters to be defined precisely, all or many of which may control the subsequent evolution

of the system. An important parameter of these disturbances is their size (radius). A tropical disturbance is conventionally defined as a region of organized convection with radius in the range of 200 to 600 km having a nonfrontal migratory character (Elsberry 1987). When such a convective disturbance either develops *in situ* or crosses a particular location, it gives rise to a convergence field whose strength and distribution depend on the size of the disturbance. It was indicated earlier by the authors (Goswami and Rao 1993, hereafter referred to as GR) that the size (radius) of the incipient vortex could be an important factor in determining the subsequent evolution of a tropical disturbance. The vortices of different size give rise to different initial convergence fields; since the process of intensification is very sensitive to the initial convergence field (Rao *et al* 1991), it is plausible that the vortices of different initial size evolve differently. The process of intensification depends both on the magnitude and distribution of heating. Besides this, cloud activity depends on the convergence field in a complicated manner; it is reasonable to expect that the dependence of the intensification on the initial vortex size does not follow a linear pattern. Given the short intensification time of the Bay cyclones in general, the influence of the initial vortex size is likely to be quite significant for the intensification process.

Recently the authors (GR) have examined the above hypothesis by using an axisymmetric model of tropical cyclone (Wada 1979). In contrast to many other axisymmetric models of tropical cyclone, Wada's model uses (a simplified) Arakawa-Schubert scheme for parameterizing convection (Arakawa-Schubert 1974). Several studies (Wada 1979; Rao *et al* 1991; Rao and Goswami 1992) have shown that Wada's model can simulate a realistic tropical cyclone, both in terms of reported observed structure (Gray 1979; Frank 1987) and in terms of comparison with results from unparameterized models (Yamasaki 1968, 1977) and detailed 3-dimensional models (Kurihara and Tuleya 1974) of tropical cyclone. Figure 1 presents a comparison between the observed structure of a mean tropical cyclone (upper panels) and the model simulated structure (lower panels). The radial-vertical cross sections of tangential wind (left panels) and the radial wind (right panels) for the mean tropical cyclone (upper panels) were adopted from Holland (1987). The lower panels show the corresponding structure for a composite Bay of Bengal cyclone. The composite was constructed by combining data from eighteen experiments: for three stations (Calcutta, Visakhapatnam and Madras), for two months (May and November) at three time steps (6^{th}, 9^{th} and 12^{th} hour) to be representative of the Bay of Bengal region. The top panels show the profiles of a mean tropical cyclone for comparison. As can be seen from these figures, allowing for individual as well as basin-wise variations, the model can capture the basic structure of a cyclone quite well. The Wada's model is therefore considered as a good research tool for studying evolution and structure of tropical cyclone.

The question that was addressed in GR was whether, given a number of incipient vortices of different size, a certain scale (size) will attain more intensity than the others. With a weak circular vortex with winds in gradient balance, a series of experiments was conducted in GR by varying r_0 – the size of the incipient vortex and T_A – the amplitude of the temperature perturbation such that all the vortices experienced the same initial central pressure drop. This was done by keeping the low level pressure at the first grid point constant for all the vortices. The range of size for the incipient vortices was taken from 100 km to 450 km to be in conformity with both observation

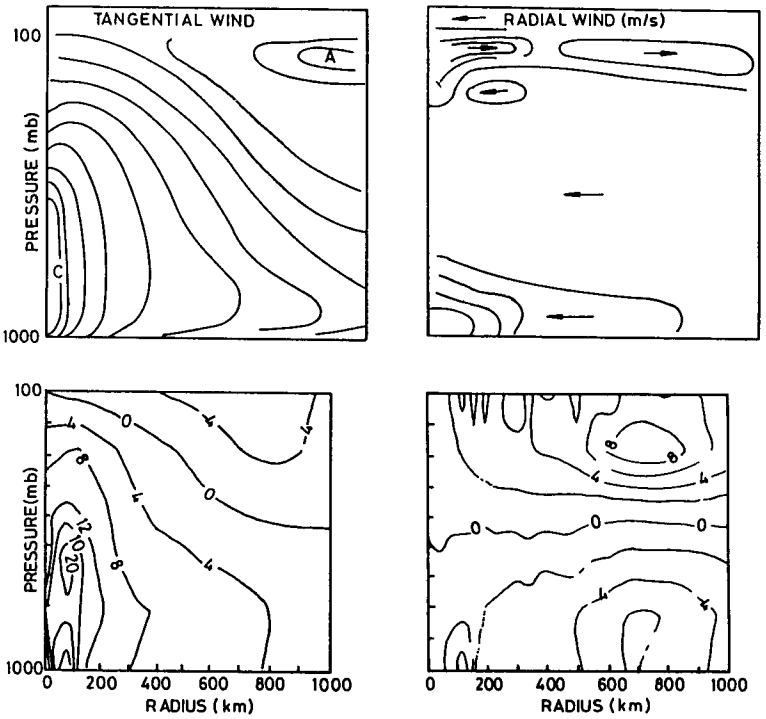

Figure 1. Comparison of structure of model simulated cyclone to that of a mean tropical cyclone. Left and right panels represent respectively, radial-vertical cross sections of tangential and radial winds (in m/s). Top panels represent structure of a mean tropical cyclone while bottom panels represent that of a model simulated cyclone constructed by taking composite of eighteen model simulations for three stations in the Bay of Bengal region: Calcutta, Madras and Visakhapatnam for the months of May and November for each station and three time steps 6^{th}, 9^{th} and 12^{th} hours respectively.

(Elseberry 1987) and numerics of the model. Eight values of r_0 were considered, starting from 100 km with an interval of about 50 km. For each case the model was then run to examine the intensification of the vortex. The intensification was measured essentially by two parameters: (1) Δp the pressure drop at the centre of the cyclone, defined as the difference between the central pressure and the ambient pressure $(p_e - p_c)$. For calculation, p_e was taken to be the lowest level pressure at 1200 km away from the centre of the vortex. (2) Maximum sustained (averaged over half an hour) low level tangential wind v_{max}. Analysis of the model results was then carried out by looking at the dependence of the intensification parameters and other dynamical fields as function of incipient vortex size r_0. The results obtained in GR showed that intensification of tropical disturbances depend on the incipient vortex size in a rather nonlinear way. The results also showed a fairly sharp selection of scale in the process of intensification. In particular, it was found that among vortices of radii ranging from 100 to 450 km embedded in the same large scale conditions, it is the vortex with radius of about 250 km that develops into the most severe system. It was also found that the process of scale selective intensification was not crucially dependent on the way one prescribed the initial state. In particular, as shown in GR,

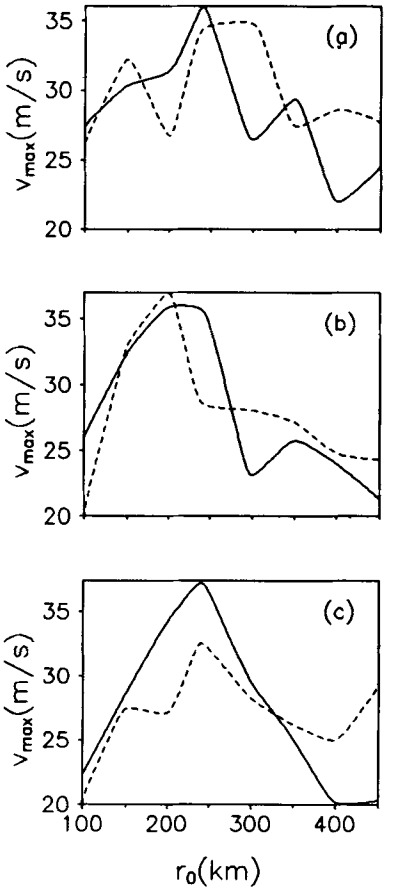

Figure 2. Sensitivity of variation of v_{max} with r_0 to initial prescription of central pressure field. Solid line represents the case when the initial central pressure drop was kept constant while the dashed line represent the results when all the vortices started with an equal value of $\frac{p(r_0)-p_c}{r_0}$. The results are presented for the month of May for three stations: (a) Calcutta, (b) Visakhapatnam and (c) Madras.

one could prescribe equal initial v_{max} for all the vortices, without affecting the scale selection. Alternatively, one could prescribe an equal initial pressure gradient field, defined by $\frac{p(r_0)-p_c}{r_0}$ where $p(r_0)$ is the pressure at the first level at $r=r_o$. The results of this experiment are presented in figure 2. In figure 2 the solid line represents the variation of v_{max} with r_0 when the initial condition was given in terms of equal p_c. The dashed line represents the same in which all the vortices started with an equal value of $\frac{p(r_0)-p_c}{r_0}$. As can be seen the essential nature of the scale selective intensification is not affected by this choice.

An analysis of a number of other derived dynamical fields was carried out in GR to establish a correspondence between a dynamical factor and scale selective intensification. It was found that low level (at 950 mb) convergence field and central cloud activity exhibit a very strong correspondence with maximum intensity attained: intensification required strong low level convergence near the centre in the initial stages (upto 6 hours). Similarly, stronger cloud activity near the centre was found to encourage intensification. It was not clear from the analysis of GR, however, as to which physical processes were key to bring about the scale selection. The purpose of the present work is to identify some of the processes that are primarily responsible for selective intensification of a particular scale. Identification of these processes will aid us in eventually developing a conceptual dynamical mechanism for scale selective intensification of tropical disturbances.

With the above objective in mind we examine the hypothesis that diffusion is likely to play an important role in the process of scale selection. The horizontal diffusion is an inherently scale dependent process. Besides, the development of the convergence and the cloud fields are likely to depend crucially on the redistribution of momentum and moisture fields by horizontal diffusion. This, in turn, may determine the organization and the extent of the central cloud activity. Very large diffusion may affect the particular organization of convective activity needed for intensification by tending to establish a horizontal homogeneity. The three processes of horizontal diffusion, viz., of momentum, moisture and heat, may not contribute equally, or in the same fashion, to the process of intensification and scale selection. The importance of the relative role of each diffusion process has also to be determined. In addition, vertical diffusion of momentum is also likely to play an important role.

In the present work the above questions are investigated by using the axisymmetric model of tropical cyclone (Wada 1979) used in GR. Experiments are carried out by varying the coefficients of horizontal diffusion of momentum (K_m), moisture (K_q), heat (K_h) and vertical (K_v). The results show that very high diffusion indeed suppresses intensification and scale selection. It was noted that the three processes of diffusion of momentum, moisture and heat do not necessarily work in the same direction. While diffusion of momentum tends to intensify small scales, diffusion of heat tends to favour intensification at larger scales. The selective intensification of vortex with radius about 250 km then appears to be a result of a delicate balance between the three diffusion processes.

2. Design of the experiments

2.1 *The basic model*

The adopted (Wada's) model is an axisymmetric model of a tropical cyclone with convection parameterized by Arakawa-Schubert scheme (Arakawa and Schubert 1974). A detailed description of the numerical model and the convective parameterization scheme can be found in earlier studies (Wada 1979; Rao *et al* 1991; Goswami and Rao 1993). We shall therefore discuss here only the essential detials of the model for the sake of completeness.

The basic equations of this symmetric model in cylindrical coordinates are as follows:

$$\frac{\partial u}{\partial t} = -\left\{u\frac{\partial u}{\partial r} + w\frac{\partial u}{\partial z}\right\} + \left\{f + \frac{v}{r}\right\}v - \theta\frac{\partial \phi}{\partial r} + K_m\left\{\nabla_1^2 - \left(\frac{1}{r^2}\right)\right\}u + \left(\frac{1}{\bar{\rho}}\right)\left\{\frac{\partial \tau_r}{\partial z}\right\}, \tag{1}$$

$$\frac{\partial v}{\partial t} = -\left\{u\frac{\partial v}{\partial r} + w\frac{\partial v}{\partial z}\right\} - \left\{f + \frac{v}{r}\right\}u + K_m\left\{\nabla_1^2 - \left(\frac{1}{r^2}\right)\right\}v + \left(\frac{1}{\bar{\rho}}\right)\left\{\frac{\partial \tau_\lambda}{\partial z}\right\}, \tag{2}$$

$$\frac{\partial \phi}{\partial z} = -\frac{g}{\theta}, \tag{3}$$

$$\frac{\partial}{\partial z}(\bar{\rho}w) = -\frac{1}{r}\frac{\partial}{\partial r}(\bar{\rho}ur), \tag{4}$$

$$\frac{\partial \theta}{\partial t} = -\left\{u\frac{\partial \theta}{\partial r} + w\frac{\partial \theta}{\partial z}\right\} + \frac{1}{\bar{\rho}\bar{\phi}}\left\{M_c\frac{\partial S}{\partial z} + D(\hat{S}_c - S - L\hat{l}_c)\right\} + \frac{LC}{\bar{\phi}} + K_h\nabla_1^2\theta + \frac{F_s}{C_P}\bar{\phi} \tag{5}$$

$$\frac{\partial \chi}{\partial t} = -\left\{u\frac{\partial \chi}{\partial r} + w\frac{\partial \chi}{\partial z}\right\} + \frac{1}{\bar{\rho}}\left\{M_c\frac{\partial \chi}{\partial z} + D(\hat{\chi}_c - \chi + \hat{l}_c)\right\} - C + K_q\nabla_1^2\chi + \frac{F_\chi}{L}, \tag{6}$$

where,

$$\phi = C_P\left\{\frac{p}{p_0}\right\}^\kappa. \tag{7}$$

The notations are given in Appendix A. The overbar denotes functions of height only, subscript c denotes the values inside clouds and the carat ($\hat{}$) denotes the values at the cloud top. For computation of frictional stress and energy and moisture fluxes the bulk aerodynamic formulae were used. Vertical structure of the model was discussed in GR.

The boundary conditions at the top and bottom are

$$w = 0 \text{ at } z = 0 \text{ and } z = Z_T$$

and the lateral boundary conditions are

$$u = v = 0 \text{ at } r = 0 \text{ and } r = r_{\max},$$

$$\frac{\partial \phi}{\partial r} = \frac{\partial \theta}{\partial r} = \frac{\partial \chi}{\partial r} = 0 \text{ at } r = 0 \text{ and } r = r_{\max}.$$

$r_{\max}$ is taken to be 12000 km to reduce the influence of lateral boundaries.

A staggered forward time differencing scheme was used while upwind differencing was used for space. The grid size in the horizontal direction is taken variable getting finer towards the centre. A choice of 49 grid points give horizontal resolution in which the grid increments near the centre is minimum (10 km) and maximum (800 km) at the distance of 12000 km. The finite difference form of equations 1, 2, 5 and 6 along with the finite difference formulation of the diffusion terms are given in Appendix B.

For convenience in computation the scalar fields of θ and ϕ are divided into two parts: an undisturbed value and a perturbed value. The hydrostatic equation is written separately as follows:

$$\theta(r,z,t) = \bar{\theta}(z) + \theta'(r,z,t), \tag{8}$$

$$\phi(r,z,t) = \bar{\phi}(z) + \phi'(r,z,t), \tag{9}$$

$$\frac{\partial \bar{\phi}}{\partial z} = -\frac{g}{\bar{\theta}}, \tag{10}$$

$$\frac{\partial \phi'}{\partial z} = -\frac{g}{\bar{\theta}}\left[\frac{\theta'}{\bar{\theta}} - \left(\frac{\theta'}{\bar{\theta}}\right)^2\right]. \tag{11}$$

2.2 *Initial conditions*

The incipient vortex, as in GR, was introduced as a circular vortex with winds in gradient balance. The strength of the incipient vortex is controlled by prescribing an initial perturbation in the temperature field of the form

$$\theta'(r,z) = T_A\left\{\cos\left(\frac{\pi r}{r_0}\right) + 1\right\}\sin\left(\frac{\pi z}{Z_T}\right) W_T(z) \quad \text{for } r \leqslant r_0$$

and

$$\theta'(r,z) = 0 \quad \text{for } r > r_0 \tag{12}$$

Here T_A is the amplitude of initial temperature perturbation and Z_T is the height of the atmosphere. The perturbation vanishes beyond $r = r_0$ with maximum at $r = 0$ and $z = \dfrac{Z_T}{2}$ if the weighting factor $W_T(z)$ were all unity. The size of the incipient vortex was identified as r_0.

The initial fields are calculated by first computing ϕ' using (11), with $\phi' = 0$ at the top. With this ϕ' field the initial tangential wind field is computed utilizing the gradient wind equation given by

$$v = \left\{-fr + r\left(f^2 + \left(\frac{4\bar{\theta}}{r}\right)\frac{\partial \phi'}{\partial r}\right)^{1/2}\right\}\Big/2 \tag{13}$$

For v to be real we must have

$$\left(f^2 + \left(\frac{4\bar{\theta}}{r}\right)\frac{\partial \phi'}{\partial r}\right) > 0 \tag{14}$$

In this model, large scale condensation occurs when the air is supersaturated. The water vapour available above the saturation value is condensed.

Experiments were conducted with mean thermodynamic states prescribed from 20 year mean climatological data for Calcutta, Visakhapatnam and Madras stations for the months of May and November to be representative of the Bay of Bengal region for these months. The choice of these mean thermodynamic states was made because about 4 – 5 times more cyclones originate over the Bay of Bengal region than over the Arabian Sea (Frank 1987). Another factor determining the choice of the mean thermodynamic states was the fact that the regional climatology of cyclogenesis over the Bay of Bengal region shows two maxima: one in the month of November and the other in the month of May (Frank 1987). Thus, strictly speaking, the results are valid only for the Bay of Bengal disturbances.

2.3 *Description of the experiments*

The basic goal of the present set of experiments is to examine the hypothesis that diffusion, which has an inherent scale dependence, is a primary source of scale selection observed in experiments carried out in GR. Besides, the four processes of diffusion viz, of momentum, moisture, heat and vertical may not contribute to the process of intensification in a simple additive fashion. While it is customary to use equal values (1000 m^2/s) for the coefficients of horizontal diffusion of momentum, heat and moisture, they can in principle be different, with significant effect on the process of intensification. Since the values of coefficients of diffusion are somewhat arbitrary, it is also important to know the extent of the effect of their variation on the process of intensification and scale selection. With these objectives in mind, two sets of experiments were carried out which we shall outline below. In the following K_m, K_q and K_h represent, respectively, the horizontal diffusion coefficients for momentum, moisture and heat while K_v represents coefficient of vertical diffusion of momentum. The effects of vertical diffusion of temperature and moisture were not included because these are considered to be small in determining the growth and structure of a tropical cyclone (Wada 1979). The experiments in GR were carried out with $K_m = K_h = K_q = K = 1000\,m^2/s$, and $K_v = 10\,m^2/s$, values that are normally adopted (Wada 1979; Ooyama 1969).

Experiment A: *Effect of variation of total diffusion*: In this series of experiments, all the three diffusion coefficients of momentum, heat and moisture were assigned the same value K. Experiments were then carried out for three different values of K and K_v; $K = 0$, $K_v = 0$ (no diffusion), $K = 1000\,m^2/s$, $K_v = 10\,m^2/s$ (standard case), and $K = 5000\,m^2/s$, $K_v = 50\,m^2/s$ (high diffusion). For each set of these values experiments were conducted for eight values of the incipient vortex size r_0, with $100 \leqslant r_0 \leqslant 450$ km and with approximately 50 km interval.

Experiment B: *Effect of variation of strength of a single diffusion process.* This series of experiments was carried out to determine the effect of a single diffusion process, either of momentum, moisture, heat or vertical. For this purpose, experiments were carried out to examine the effect both in the absence and in the presence of the other diffusion processes.

The first set of experiments was conducted by switching off any three diffusion processes (say moisture, heat and vertical) and varying the fourth (in this case K_m). This process was repeated for each K_m, K_q, K_h and K_v with the same set of values

for r_0 as in experiment A. The second set of experiments was conducted keeping the other diffusion strengths at moderate values.

3. Results

3.1 *Effect of variation of total diffusion*

Figure 3 shows the effect of variation of the strength of total (horizontal as well as vertical) diffusion on the intensification of Bay of Bengal disturbances. In this figure upper (a, b), middle (c, d) and lower (e, f) panels show, respectively, the intensification

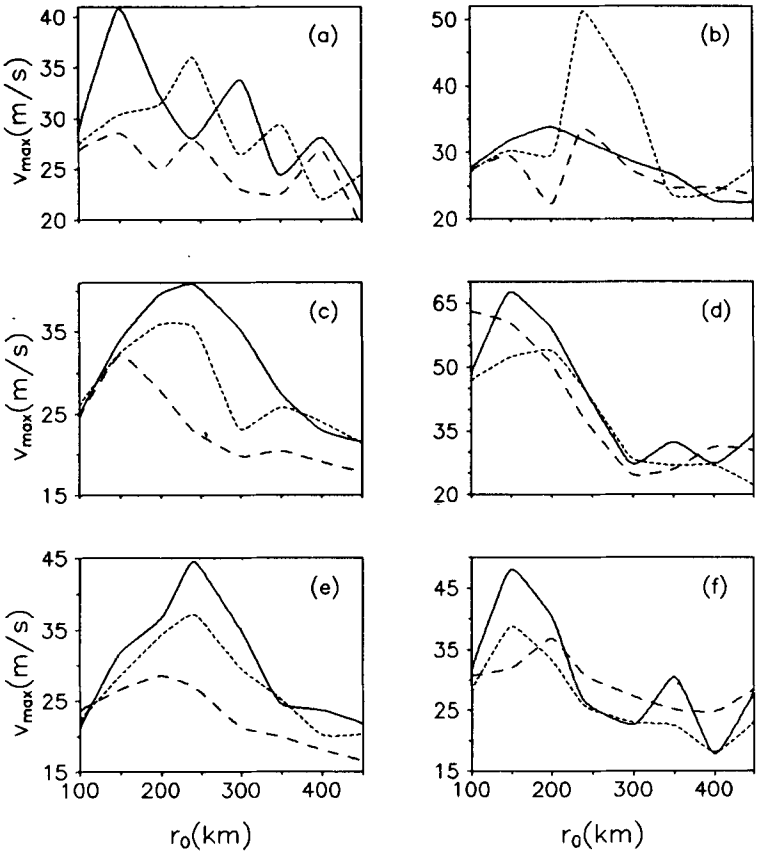

Figure 3. Effect of variation of total diffusion on the size dependent intensification of tropical disturbances.

Upper (a, b), middle (c, d) and lower (e, f) panels represent, respectively, intensification versus size of incipient vortex for the stations Calcutta, Visakhapatnam and Madras. Left panels, (a, c, e) represent results for the month of May while the right panels (b, d, f) represent those for November. In each panel solid lines show the pattern for diffusionless case ($K_m = K_q = K_h = K_v = 0$), small dash lines for moderate diffusion case ($K_m = K_q = K_h = 1000\,m^2/s$; $K_v = 10\,m^2/s$) and big dash lines for high diffusion case ($K_m = K_q = K_h = 5000\,m^2/s$; $K_v = 50\,m^2/s$). In each panel radius (r_0) in kms of the incipient vortex is given along x-axis and maximum lowlevel tangential velocity (v_{max}) attained is given along y-axis in m/s.

pattern for the stations Calcutta, Visakhapatnam and Madras. Left panels (a, c, e) of this figure represent the results for the month of May while the right panels (b, d, f) show the corresponding results for November. Solid lines in each panel represent diffusionless case while small dashed and big dashed lines represent for moderate and high diffusion cases, respectively. In each panel radius (r_0) in kms of the incipient vortex is given along x-axis and maximum low level tangential velocity (v_{max}) in m/s attained is given along y-axis.

It can be seen from figure 3, that diffusion plays a significant role in the intensification of disturbances. In general the intensity reduces as we go from low diffusion to higher diffusion, especially at smaller scales. This change is, however, not linear, and for certain mean thermodynamic state may show reverse trend (e.g. figure 3f). In the case of high diffusion (big dashed line) the intensification reduces drastically. However,

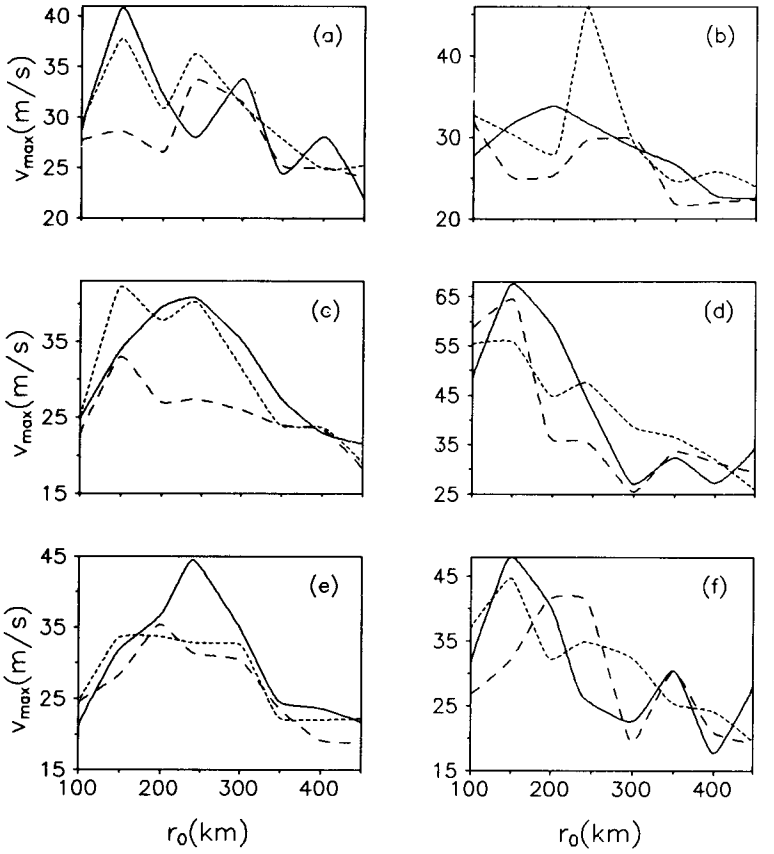

Figure 4. Effect of variation of only momentum diffusion in the absence of other diffusion processes.

Upper (a, b), middle (c, d) and lower (e, f) panels represent respectively intensification as a function of r_0 for the stations Calcutta, Visakhapatnam and Madras. Left panels (a, c, e) represent for the month of May while right panels (b, d, f) for November. Solid lines in each panel represent for zero momentum diffusion ($K_m = 0$), small dash line for moderate diffusion ($K_m = 1000\,m^2/s$) and big dash line for high diffusion ($K_m = 5000\,m^2/s$). K_q, K_h and K_v are kept at zero.

more than the intensity it is the scale selection process that is affected by high diffusion. Though it seems to prefer lower scales, the scale selection itself is nearly absent. The effect of diffusion also seems to depend on the mean thermodynamic state, as can be seen from figure 3 d, f. In the cases of low and medium diffusion the highest intensity is attained at smaller scales ($r_0 \simeq 150 - 250$ km) in the month of November while in the high diffusion case intensities seem to be comparable with those for the cases of zero and medium diffusion, especially at higher scales. In the month of May the scale selection is at intermediate scales ($r_0 \simeq 250$ km) for low and medium diffusion cases and at smaller scales for high diffusion cases. Comparison of left and right panels shows that intensities in the month of November are higher than those of May in all the cases, especially at lower scales.

3.2 *Effect of variation of a single diffusion process*

In this set of experiments the role of variation of a single diffusion process, be it of momentum, moisture, heat or vertical diffusion has been studied. Figures 4, 5, 6 and 7 show respectively the effect of only momentum, only moisture, only heat and only

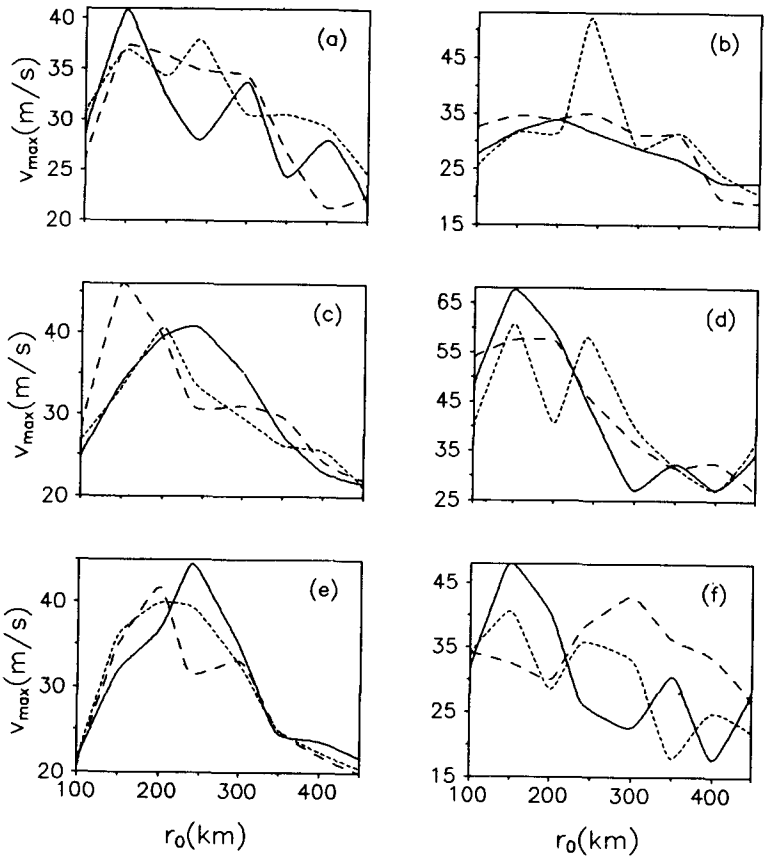

Figure 5. Same as figure 4 but for moisture diffusion. Here $K_m = K_h = K_v = 0$ and K_q is given the values 0 (solid lines), 1000 m^2/s (small dash line) and 5000 m^2/s (big dash line).

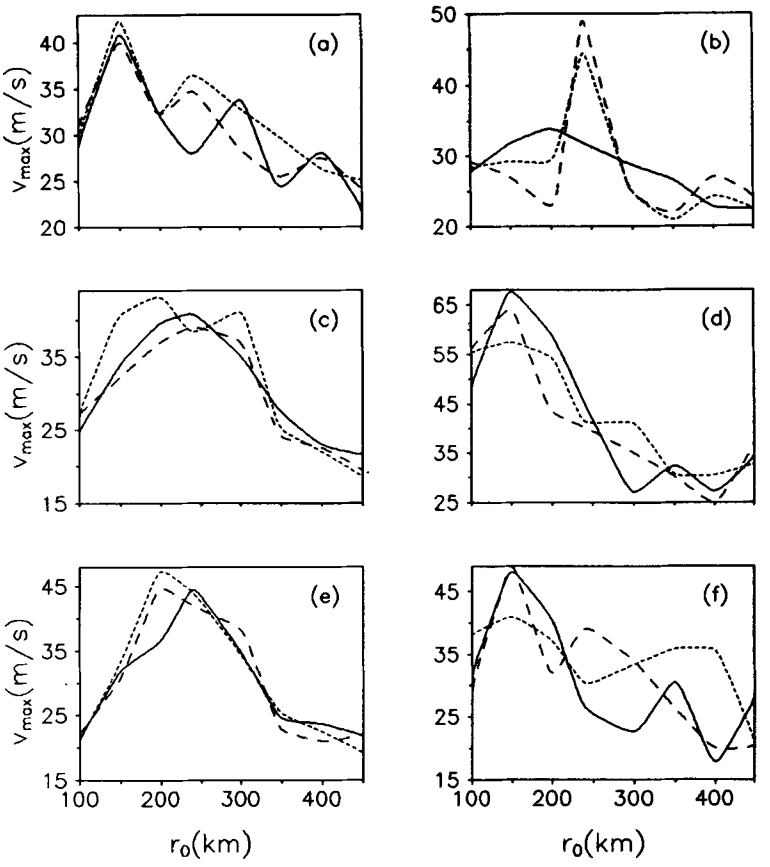

Figure 6. Same as figure 4 but for heat diffusion. Here $K_m = K_q = K_v = 0$ and K_h is given the values 0 (solid lines), 1000 m^2/s (small dash line) and 5000 m^2/s (big dash line).

vertical diffusion process on the intensification of Bay of Bengal disturbances in the absence of other diffusion processes while figures 8, 9, 10 and 11 show the effect of a single diffusion in the presence of the other diffusion processes at moderate values.

3.2.1 *In the absence of other diffusion processes*

Figures 4, 5, 6 and 7 show respectively the effect of variation of only momentum, only moisture, only heat and only vertical diffusion process on the intensification of Bay of Bengal disturbances in the absence of other diffusion processes. In these figures upper (a, b), middle (c, d) and lower (e, f) panels show respectively the intensification pattern for the stations Calcutta, Visakhapatnam and Madras. Left panels (a c, e) of this figure represent the results for the month of May while the right panels (b, d, f) represent those for November. Solid lines in each panel represent the results for zero diffusion case while small dashed and big dashed lines represent the moderate and high values of the corresponding diffusion cases, respectively.

It can be seen from figure 4 that the presence of high horizontal momentum diffusion (big dash line) reduces the intensity, especially at smaller scales and suppresses the

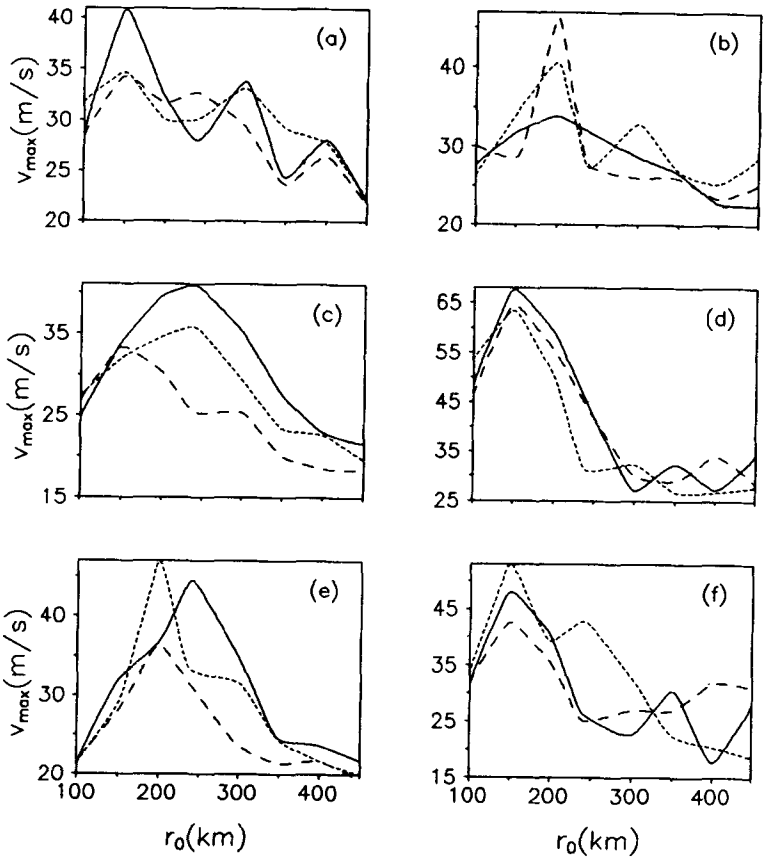

Figure 7. Same as figure 4 but for vertical diffusion. Here $K_m = K_q = K_h = 0$ and K_v is given the values 0 (solid lines), 10 m^2/s (small dash line) and 50 m^2/s (big dash line).

scale selection in general. In the case of no diffusion (solid line), maximum intensities are attained at lower scales ($r_0 \leqslant 250$ km) while moderate diffusion (small dashed line) also prefers lower scales but reduces the sharpness of the scale selection process. This figure also shows that for higher scale disturbances ($r_0 \geqslant 300$ km), the intensification is more or less insensitive to the variation of horizontal momentum diffusion. Variation of only moisture diffusion (figure 5) does not affect the intensification in general but reduces the sharpness of the scale selection as we increase the diffusion. It should be noted, however, that in contrast to variation of horizontal diffusion of momentum (figure 4), which affects the smaller scales more than the larger scales, the effect of variation of moisture diffusion is more or less uniform with scale. From figure 6, it can also be seen that the variation of only heat diffusion does not affect the intensification, in general. However, as can be seen from the left panels, the presence of only moderate heat diffusion favours intensification, especially at smaller scales in the month of May while low and high diffusion favours larger scale disturbances in the month of November. Figure 7 shows that the vertical diffusion does not significantly affect the nature of scale selection. However, high vertical diffusion reduces the intensification in general and shifts the scale selection to lower scales.

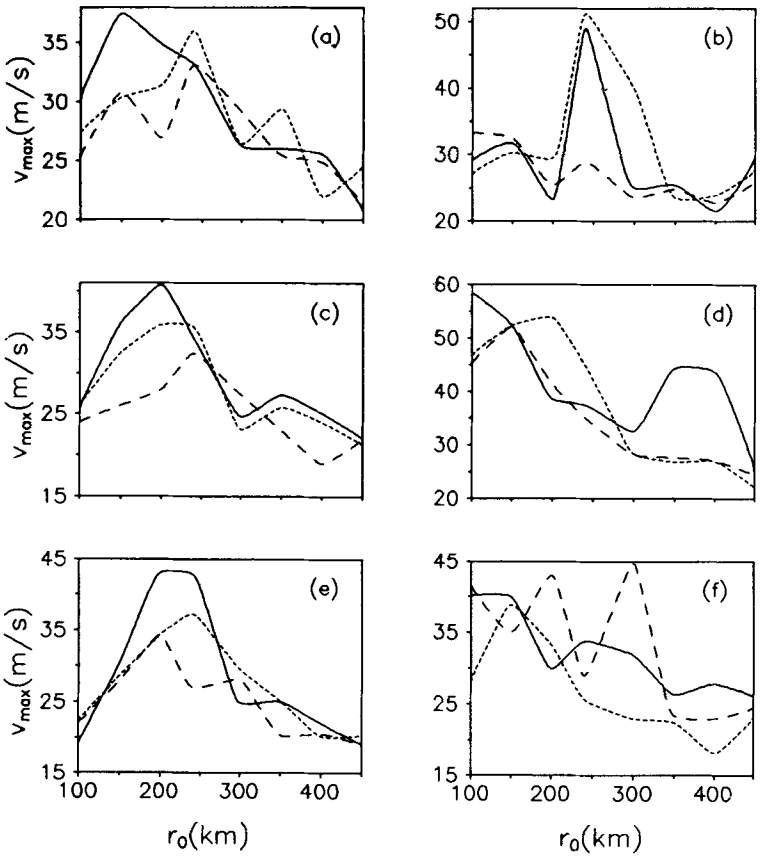

Figure 8. Effect of variation of only horizontal momentum diffusion in the presence of other diffusion processes.

Upper (a, b), middle (c, d) and lower (e, f) panels represent respectively, intensification pattern for the stations Calcutta, Visakhapatnam and Madras. Left panels (a, c, e) represent for the month of May while right panels (b, d, f) for November. K_q, K_h and K_v are kept at moderate values and K_m is given the values 0 (solid line), 1000 m^2/s (small dash line) and 5000 m^2/s (big dash line).

3.2.2 *Variation of a single diffusion strength in presence of other diffusion processes*

Figures 8, 9, 10 and 11 show respectively the effect of only momentum, only moisture, only heat and only vertical diffusion process on the intensification of Bay of Bengal disturbances in the presence of other diffusion processes. In these figures upper (a, b), middle (c, d) and lower (e, f) panels show, respectively, the intensification patterns for the stations Calcutta, Visakhapatnam and Madras. Left panels (a, c, e) of these figures represent results for the month of May while the right panels (b, d, f) represent those for November. In each panel, solid, small dashed and big dashed lines represent the results for zero, moderate and high values of the particular diffusion process, respectively. In each case, the constant diffusion processes are kept at their corresponding standard strengths.

Figure 8 shows that high horizontal momentum diffusion (big dashed lines) reduces the intensification, especially at intermediate scales and suppresses the sharpness of

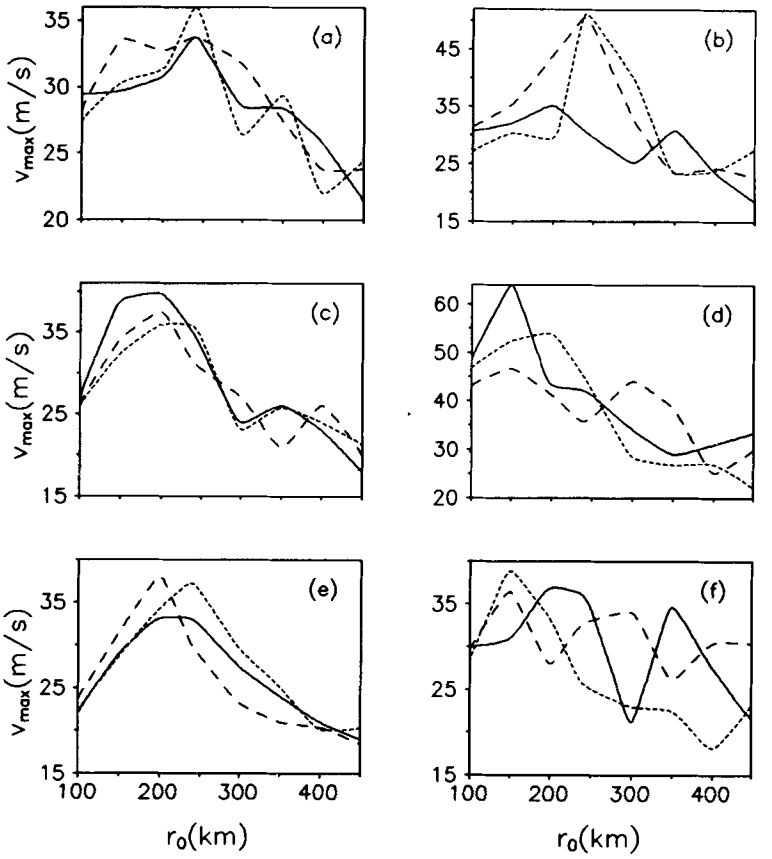

Figure 9. Same as figure 8 but for moisture diffusion. Here $K_m = K_h = 1000\,m^2/s$; $K_v = 10\,m^2/s$ and K_q is given the values 0 (solid line), $1000\,m^2/s$ (small dash line) and $5000\,m^2/s$ (big dash line).

the scale selection. It also shows that the absence of horizontal diffusion (solid line) process favours intensification at smaller scales in general. Figure 9 reveals that variation of moisture diffusion does not affect intensification pattern significantly. Although high moisture diffusion (big dashed line) favours intensification at smaller scales, intensification is insensitive to variation in the strength of moisture diffusion at higher scales. It may be noted from figure 10, which shows the effect of variation of heat diffusion process, that high diffusion (big dashed line) favours intensification, especially at smaller scales while the diffusionless case favours higher scale disturbances. In contrast to the other diffusion processes, increasing values of horizontal diffusion of heat increases the intensification of the disturbances, especially in the lower scales.

In presence of moderate horizontal diffusion, as can be seen from figure 11, the absence of vertical diffusion (solid lines), favours scale selection at smaller scales and reduces the sharpness of the scale selection while in the case of moderate diffusion (small dashed lines) there is a sharper scale selection at about 250 km. The high vertical diffusion (big dashed lines) reduces the intensification and the maximum

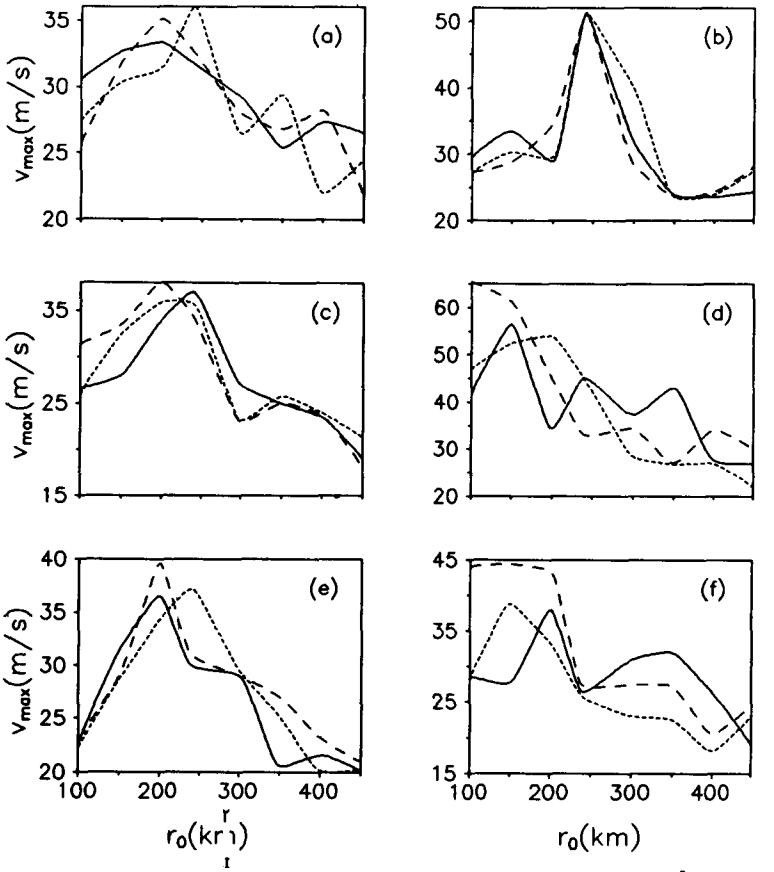

Figure 10. Same as figure 8 but for heat diffusion. Here $K_m = K_q = 1000\,m^2/s$; $K_v = 10\,m^2/s$ and K_h is given the values 0 (solid line), $1000\,m^2/s$ (small dash line) and $5000\,m^2/s$ (big dash line).

intensities in this case are attained at smaller scales and generally reduces the sharpness of the scale selection.

4. Conclusions

A synthesis of the results from the above experiments may be summarised as follows:

- The process of scale selective intensification may exist even without diffusion, although the process of selection is somewhat weak in the absence of diffusion.
- Diffusion generally suppresses intensification (figure 3). High diffusion also suppresses scale selection.
- From the small dash lines of figures 4, 5, 6 and 7, it may be noted that the presence of only a single diffusion process of moderate strength either of momentum or heat or vertical, favours intensification at smaller scales while the presence of only moderate moisture diffusion favours relatively higher scales. The sharpness of the scale selection is however, greatly reduced in all the cases. So it may be concluded

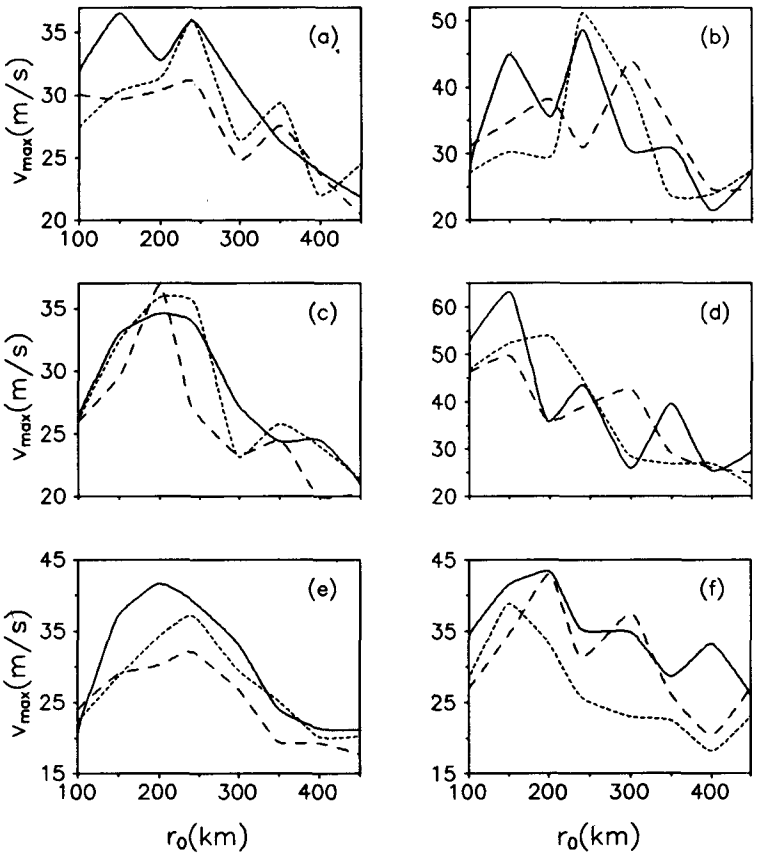

Figure 11. Same as figure 8 but for vertical diffusion. Here $K_m = K_q = K_h = 1000\,m^2/s$ and K_v is given the values 0 (solid line), $10\,m^2/s$ (small dash line) and $50\,m^2/s$ (big dash line).

that no single individual diffusion process can give rise to a sharp scale selection at $r_0 = 250$ km.

- A comparison of the solid lines in figure 4 (zero total diffusion) and figure 8 (absence of only horizontal diffusion) shows that absence of horizontal diffusion favours intensification at smaller scales, in general.
- Comparison of figures 8, 9, 10 and 11 shows that, in the absence of horizontal momentum diffusion or vertical diffusion the intensities of the disturbances are relatively high. It can also be seen from figures 8 and 11 that high values of horizontal and vertical momentum diffusions (big dashed lines) reduce intensification in general and prefer intermediate scale disturbances for intensification. So it may be concluded that momentum diffusion in general reduces intensification and favours the scale selection at about 250 km.
- Variation of the moisture diffusion does not affect the intensification pattern in general. However, it affects the sharpness of scale selection.
- It can be seen from figures 6 and 10 that intensities of the disturbances increase with strength of heat diffusion, especially in the presence of other diffusion processes. High values of heat diffusion shift the scale selection to lower scales.

The present work therefore points to the process of diffusion as a major factor in bringing about scale selective intensification. It must be remembered, however, that the inclusion of horizontal as well as vertical diffusion in the present model is somewhat crude; both are represented by constant eddy viscosity coefficients. While in the vertical it is desirable to use a sophisticated formulation of the boundary layer processes, with a z-dependent eddy viscosity coefficient, a (horizontal) resolution-dependent coefficient of diffusion can be used in the radial direction. However, we note from the results of Part I of this work (GR) that the factors that are crucial for intensification are core ($r < 300$ km) convergence and cloud fields. For radial distances of this order our horizontal grid spacing is essentially constant. Thus the assumption of a constant coefficient of horizontal diffusion is not likely to be a severe one. It should be mentioned that the present model uses upwind difference scheme in the horizontal direction and hence suffers from the inherent weakness of implicit diffusion of upwind differencing. Considering the sensitivity of our results to the process of diffusion and problems inherent in modelling diffusion with upwind differencing, we feel an important next step should be to verify our results with a different model, perhaps a three-dimensional limited area model. In all the cases presented here, the intensification time (time taken to reach maximum low level tangential velocity) is rather small – of the order of 12 hours. However, in many areas the intensification takes a much longer time, of the order of 48 hours. Thus for these systems diffusion will have much longer time to act. Thus the present results which are essentially valid for the Bay of Bengal depressions may not be valid for other tropical regions in general. Experiments to investigate scale selective intensification for other basins are in progress.

Appendix A: Notation

C	: large scale condensation per unit time and per unit mass.
C_P	: specific heat of dry air at constant pressure.
D	: suffix indicating detrainment level.
F_s, F_χ	: Air-sea exchange of sensible heat and water vapour respectively, from the surface to the atmosphere.
f	: Coriolis parameter.
g	: acceleration due to gravity.
K_m, K_q, K_h	: coefficients of horizontal diffusion of momentum, moisture and heat, respectively.
τ_r, τ_λ	: radial and tangential vertical turbulent stresses.
L	: latent heat of condensation of water vapour.
$M_c(z)$	: total vertical cloud mass flux at level z.
T_A	: temperature perturbation to generate the incipient vortex.
r, λ	: suffixes indicating radial and tangential directions, respectively.
r_0	: incipient vortex size (radius).
S	: dry static energy.
u, v, w	: radial, tangential and vertical components of velocity.
ρ	: density of air.
ρ_s	: density of air at the surface.
χ	: mixing ratio of water vapour.

κ : (R/C_p).
l_c : liquid water content of the cloud.
θ : potential temperature.
$W_T(Z)$: weighting factor.
∇_1^2 : $\partial^2/\partial^2 r + 1/r\partial/\partial r$.

Appendix B

Time staggering was used to avoid the appearance of computational mode in time. u, v and w are defined at time $(t+\frac{1}{2})\Delta t$, while θ, q and ϕ are defined at time $t\ \Delta t$, where Δt is the time increment and t is the time level. For advection and diffusion terms forward differencing was used. The finite difference representations for the time derivatives are given as follows:

$$\frac{u^{t+(1/2)}-u^{t-(1/2)}}{\Delta t} = -\left[u\frac{\partial u}{\partial r}+w\frac{\partial u}{\partial z}-\left(f+\frac{v}{r}\right)v\right]^{t-(1/2)}-\left[\theta\frac{\partial \phi}{\partial r}\right]^{t}$$
$$+\left[K_m\left(\nabla_1^2-\frac{1}{r^2}\right)u+\frac{1}{\bar\rho}\frac{\partial \tau_r}{\partial z}\right]^{t-(1/2)}$$

$$\frac{v^{t+(1/2)}-v^{t-(1/2)}}{\Delta t} = -\left[u\frac{\partial v}{\partial r}+w\frac{\partial v}{\partial z}-\left(f+\frac{v}{r}\right)u\right]^{t-(1/2)}$$
$$+\left[K_m\left(\nabla_1^2-\left(\frac{1}{r^2}\right)\right)v+\frac{1}{\bar\rho}\frac{\partial \tau_\lambda}{\partial z}\right]^{t-(1/2)}$$

$$\frac{\theta^t-\theta^{t-1}}{\Delta t} = -u^{t-(1/2)}\frac{\partial \theta^{t-1}}{\partial r}+w^{t-(1/2)}\frac{\partial \theta^{t-1}}{\partial z}+\frac{1}{\bar\rho\phi}$$
$$\left\{M_c^{t-(1/2)}\frac{\partial S^{t-1}}{\partial z}+D^{t-(1/2)}(\hat S_c-S-L\hat l_c)^{t-1}\right\}$$
$$+\frac{LC^{t-1}}{\bar\phi}+K_h\nabla_1^2\theta^{t-1}+\frac{F_\beta^{t-(1/2)}}{C_p\bar\phi}$$

$$\frac{\chi^t-\chi^{t-1}}{\Delta t} = -u^{t-(1/2)}\frac{\partial \chi^{t-1}}{\partial r}+w^{t-(1/2)}\frac{\partial \chi^{t-1}}{\partial z}+\frac{1}{\bar\rho}$$
$$+\left\{M_c^{t-(1/2)}\frac{\partial \chi^{t-1}}{\partial z}+D^{t-(1/2)}(\hat\chi_c-\chi+\hat l_c)^{t-(1/2)}\right\}$$
$$-C^{t-1}+K_q\nabla_1^2\chi^{t-1}+\frac{F_\chi^{t-1}}{L}$$

References

Arakawa and Schubert W H 1974 Interaction of a cumulus cloud ensemble with the large scale environment, Part-I; *J. Atmos. Sci.* **31** 674–701

Elseberry R L 1987 Observation and analysis of tropical cyclone motion; *A global view of tropical cyclones* (ed.) R L Elseberry (University of Chicago Press) pp 1–12

Frank W M 1987 Tropical cyclone formation; *A global view of tropical cyclones* (ed.) R L Elseberry (University of Chicago Press) pp 53–90

Goswami P and Rao R K 1993 Incipient vortex size dependent evolution of tropical disturbances. Part I Results from a numerical experiment; *Proc. Indian Acad. Sci. Earth and Planet. Sci.* **102** 439–463

Gray W M 1979 Hurricanes: their formation, structure and likely role in the tropical circulation, in Meteorology over the tropical oceans; *Royal Meteor Soc.* James Glaisher House, Grenville Place, Bracknell, Bewrkshire, RG12 IBX, 155–218

Holland G J 1984 Mature structure and structure change in A global view of tropical cyclones (ed), R L Elseberry (University of Chicago Press) pp. 13–52

Kurihara Y and Tuleya R E 1974 Structure of a tropical cyclone developed in a three dimensional numerical simulation model; *J. Atmos. Sci.* **31** 893–919

Ooyama K 1969 Numerical simulation of the life cycle of tropical cyclones; *J. Atmos Sci.* **26** 3–40

Rao M S, Goswami P and Nagaraj Upadhyaya H V 1991 On the Gross Predictability of Monsoonal Depressions; *Proc. Indian Acad. Sci., Earth Planet. Sci.* **100**, 127–144

Rao R K and Goswami P 1992 Simulation of the evolution and structure of a tropical cyclone using an axisymmetric model. IITK and C-MMACS internal report (Dept. of Physics, Indian Institute of Technology, Kanpur, Kanpur 208 016, India)

Southern R L 1987 Tropical cyclone warning and mitigation systems; *A global view of tropical cyclones* (ed) R L Elseberry (University of Chicago Press) pp. 147–184

Wada M 1979 Numerical experiments of the tropical cyclone by using the Arakawa-Schubert parameterization, *J. Meteorol. Soc. Japan* **57**, 505–530

Yamasaki M 1968 Numerical simulation of tropical cyclone development with the use of primitive equations; *J. Meteorol. Soc. Japan*, **46**, 178–201

Yamasaki M 1977 A preliminary experiment of the tropical cyclone without parameterizing the effects of cumulus convection; *J. Meteorol. Soc. Japan*, **55**, 11–31